RESEARCH ARTICLE

Figures and figure supplements

The transcription factor Xrp1 is required for PERK-mediated antioxidant gene induction in *Drosophila*

Brian Brown *et al*

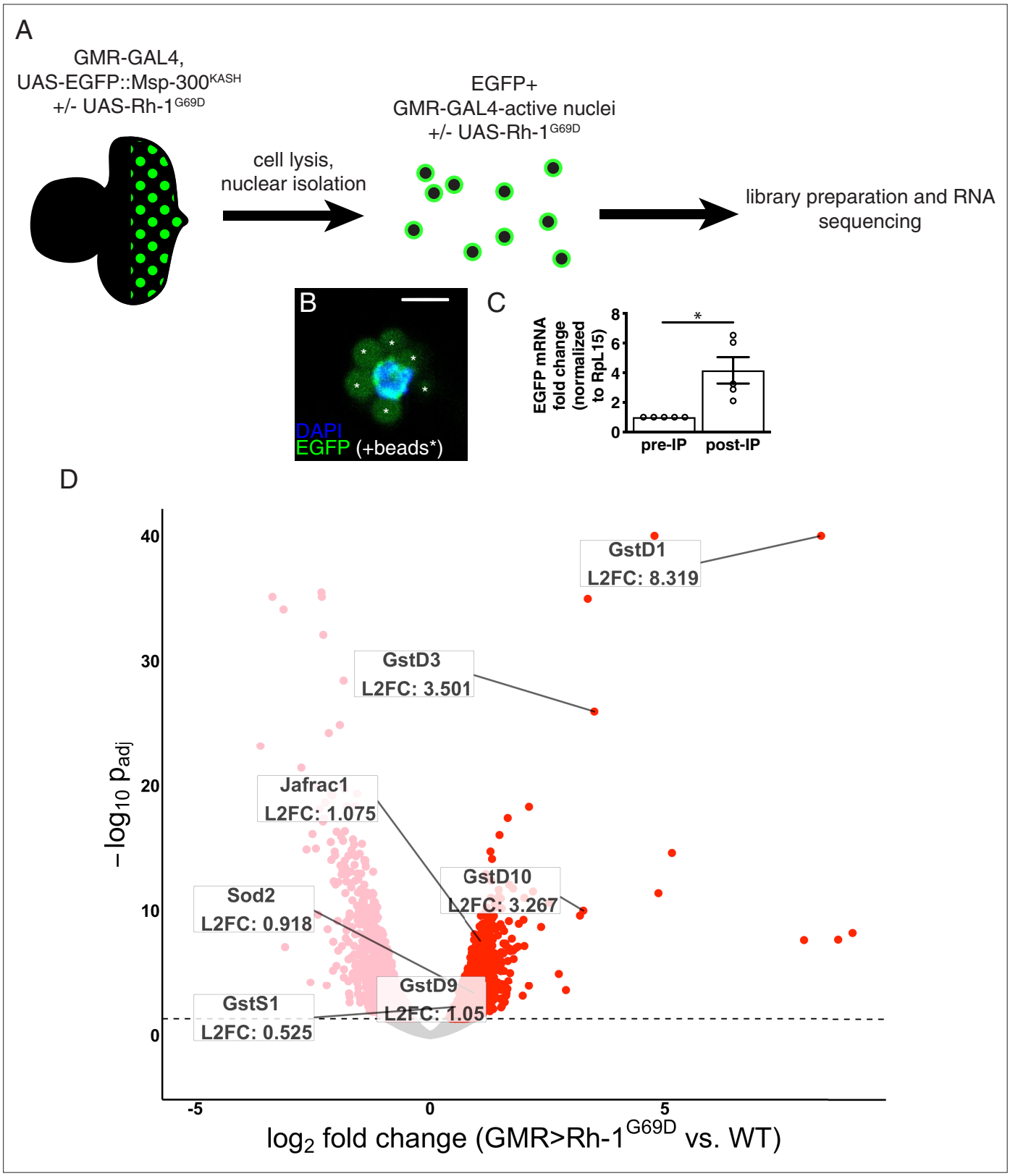

Figure 1. *RNA-sequencing reveals upregulation of antioxidant genes in response to ER stress.* (**A**) Workflow for isolation of tagged nuclei from eye imaginal discs and preparation of total RNA for transcriptional profiling. (**B**) A representative image of an isolated, EGFP-tagged nucleus. Asterisks label auto-fluorescent anti-EGFP-coupled beads. Scale bar = 5 μm. (**C**) Representative qRT-PCR of pre- and post-isolation disc nuclei showing a significant enrichment of EGFP mRNA following isolation. The error bar represents standard error (SE). Statistical significance was assessed through a two

Figure 1 continued on next page

Figure 1 continued

tailed t-test. * = $p < 0.05$. (**D**) Volcano plot of genes differentially expressed in the presence or absence of $Rh1^{G69D}$ expression. Genes significantly up/downregulated in response to $Rh1^{G69D}$ are shown in red and pink, respectively. A select set of antioxidant genes induced by $Rh1^{G69D}$ are labeled with their $\log_2$ fold change values. Note: $-\log_{10} p_{adj}$ of *gstD1* exceeded the bounds of the graph (180) and was constrained to the maximum displayed value of 40 for readability.

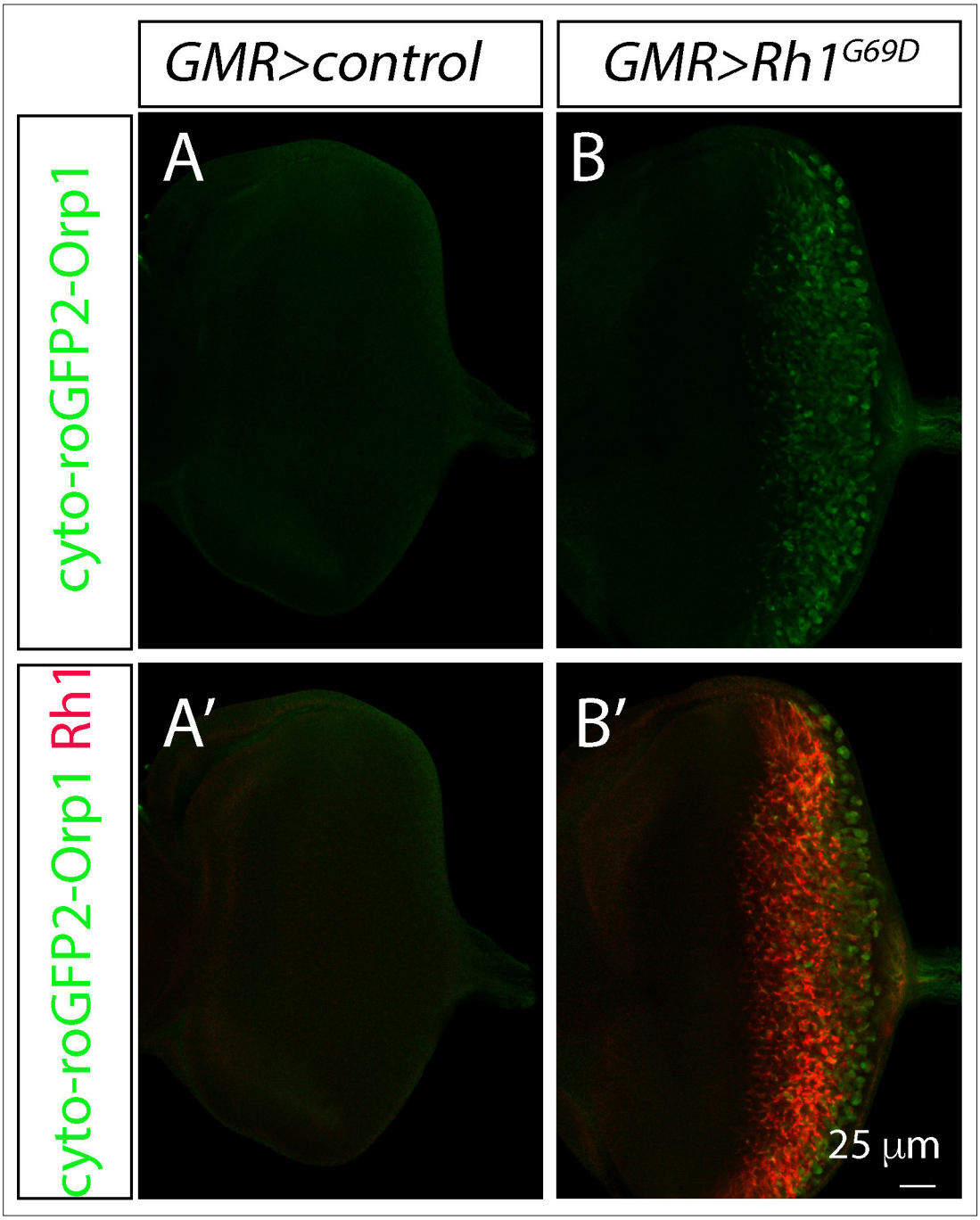

Figure 1—figure supplement 1. *Evidence for ROS build up in eye discs expressing Rh1^{G69D}.* Representative eye imaginal discs expressing the cytosolic ROS sensor cyto-roGFP2-Orp1. The expression of this reporter was driven by *GMR-Gal4* either alone (**A**), or together with *UAS-Rh1^{G69D}*. (**A, B**) show GFP single channel images, and (**A′, B′**) show merged channels with anti-Rh1 (red).

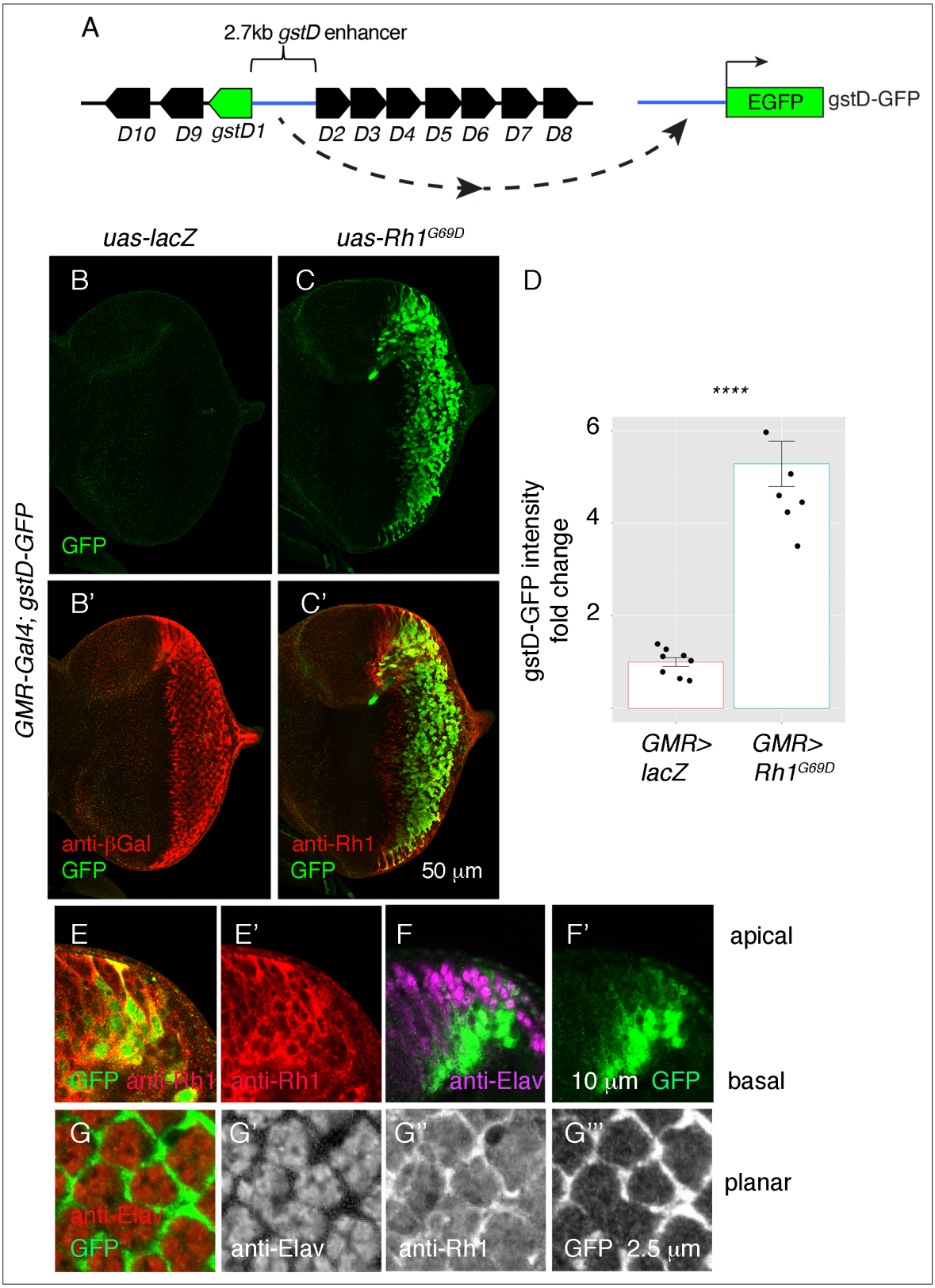

Figure 2. *ER stress induces gstD-GFP expression in the eye imaginal disc.* (**A**) Schematic of the *gstD-GFP* reporter and the *gstD* locus, which encodes multiple *gstD* isozymes in close proximity to the 2.7 kb *gstD1/gstD2* intergenic enhancer (scale is approximate). (**B–C**) Planar views of *gstD-GFP* larval eye discs also expressing either *lacZ* or $Rh1^{G69D}$ driven by *GMR-Gal4*. (**B', C'**) show merged images of discs with *gstD-GFP* expression in green, and Rh1 or lacZ in red. (**B, C**) show only the green channel. Anterior is to the left and posterior to the right. Scale bar = 50 μm. (**D**) Quantification of gstD-GFP

Figure 2 continued on next page

Figure 2 continued

pixel intensity fold change from eye discs with the indicated genotypes. Statistical significance based on t test (two tailed). **** = $p < 0.0001$. (**E, F**) A magnified view of *GMR > Rh1^{G69D}* eye discs in apico-basal orientation. gstD-GFP signals are marked in green. (**E**) Posterior eye disc double labeled with anti-Rh1 (red). (**F**) An equivalent region labeled with anti-Elav antibody that marks photoreceptors (magenta). Scale bar = 10 μm (**G**) A magnified view of *GMR > Rh1^{G69D}* eye discs in planar orientation with gstD-GFP (green) and anti-Elav labeling (red). Individual channels are shown separately in (G' – G'''). Scale bar = 2.5 μm.

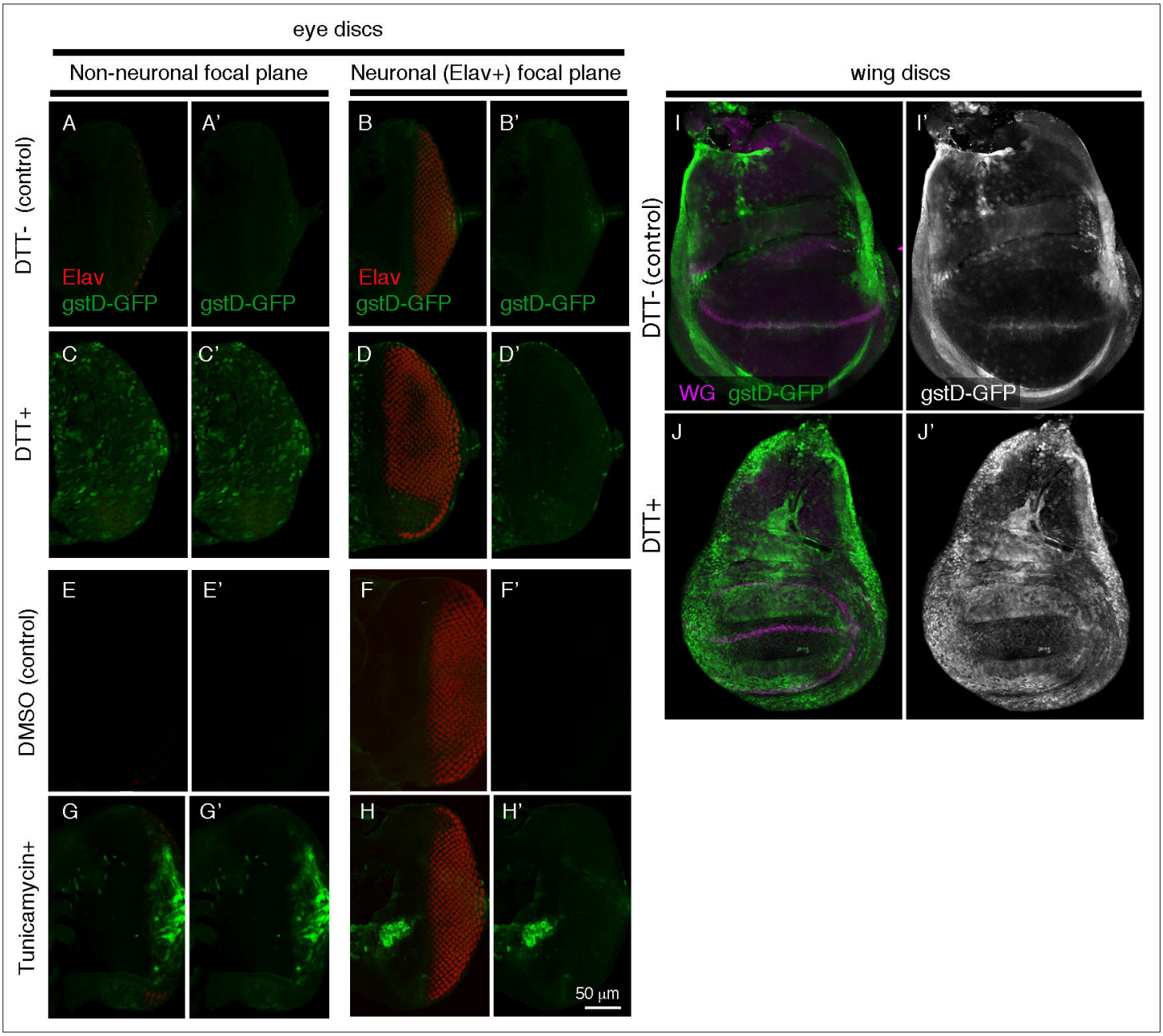

Figure 2—figure supplement 1. *gstD-GFP induction by ER-stress causing chemicals. gstD-GFP* transgenic larval imaginal discs, imaged for gstD-GFP (green). (**A–D**) Representative images of eye imaginal discs incubated in control culture media (**A, B**), or with that containing the ER-stress-causing chemical DTT (**C, D**). Anti-Elav (red) labeling shows photoreceptor nuclei. Shown are images of two different focal planes: (**A, C**) The support cell layer focal plane that does not include Elav-positive nuclei. (**B, D**) The Elav-positive focal plane. Note that gstD-GFP is induced primarily in the Elav-negative cell layer. (**E, H**) Eye discs incubated with tunicamycin dissolved in DMSO (**G, H**), or just with DMSO (**E, F**). Shown are two different focal planes, the Elav-negative (**E, G**) and Elav-positive cell layers (**F, H**). (**I, J**) Wing imaginal discs incubated with control culture media (**I**), or with media containing 2 mM DTT for 4 hr (**J**). Anti-Wg (magenta) was used for counterstaining. (**A', B', C', D', E', F', G', H', I', J'**) gstD-GFP single channels. Scale bar in H' = 50 µm.

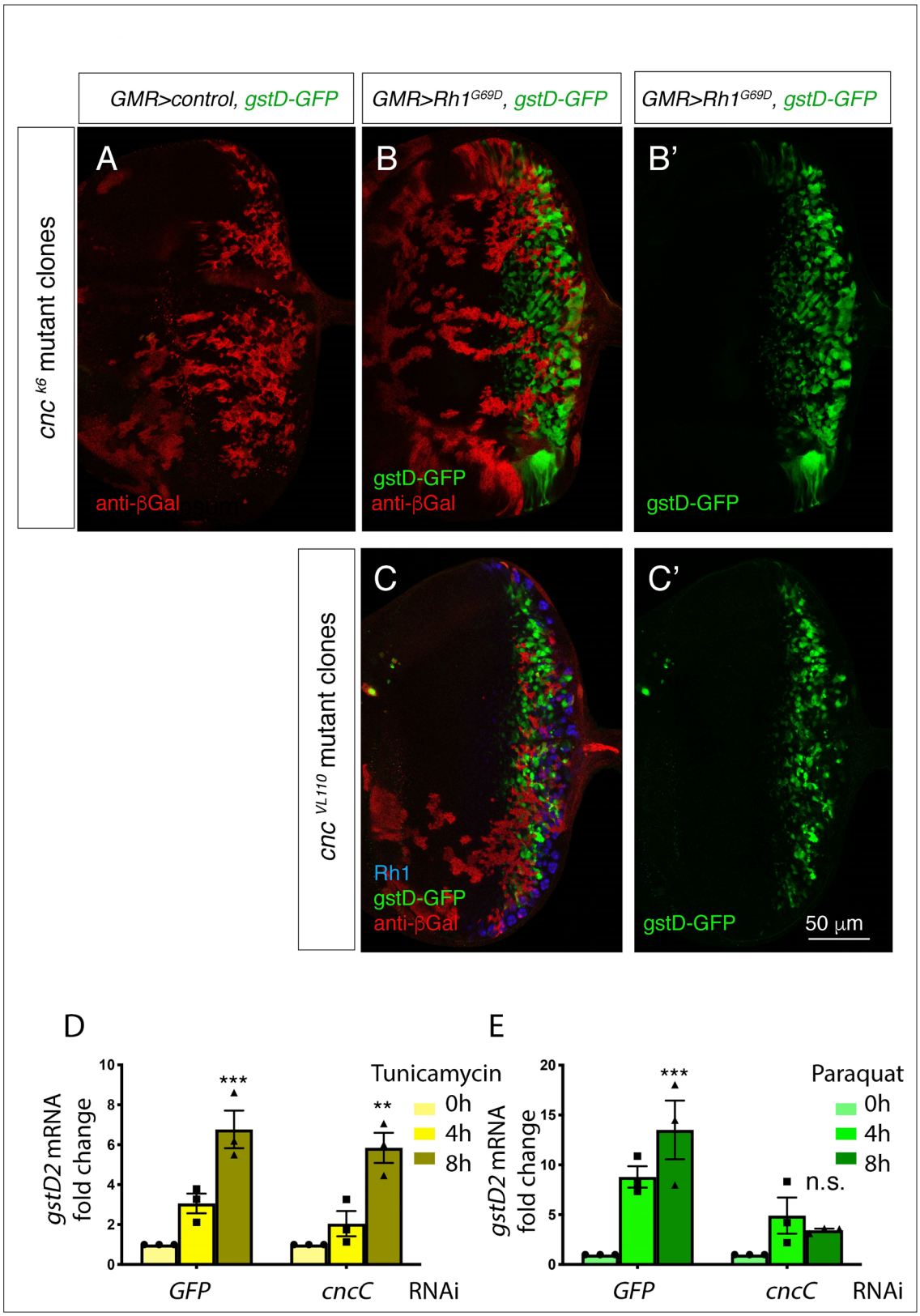

Figure 2—figure supplement 2. *ER stress-induced expression of gstDs is independent of cncC.* (**A–C**) Eye imaginal discs labeled with gstD-GFP (green). The *cncC* homozygous mosaic clones are marked by the absence of anti- β Gal antibody labeling (red). (**A**) A control disc with *cnc*^{k6} mutant clones but not overexpressing *Rh1*^{G69D}. (**B, C**) *GMR> Rh1*^{G69D} eye discs with *cncC* mutant clones. Note that gstD-GFP signal is present in *cnc*^{k6} (**B**) nor *cnc*^{vl100} homozygous mutant clones. In (**C**), blue shows anti-Rh1. (**B', C'**) show gstD-GFP only channels of (**B, C**). (**D, E**) qRT-PCR of *gstD2* normalized

Figure 2—figure supplement 2 continued on next page

Figure 2—figure supplement 2 continued

to *Rpl15* in S2 cells where ER stress is induced by 10 µg/ml tunicamycin treatment (**D**) or 20 mM paraquat (**E**) for 0, 4, or 8 hr. Cells were treated with dsRNA against either *GFP* or *cncC*. Scale bar = 50 um. ** = $p < 0.005$, *** = $p < 0.001$.

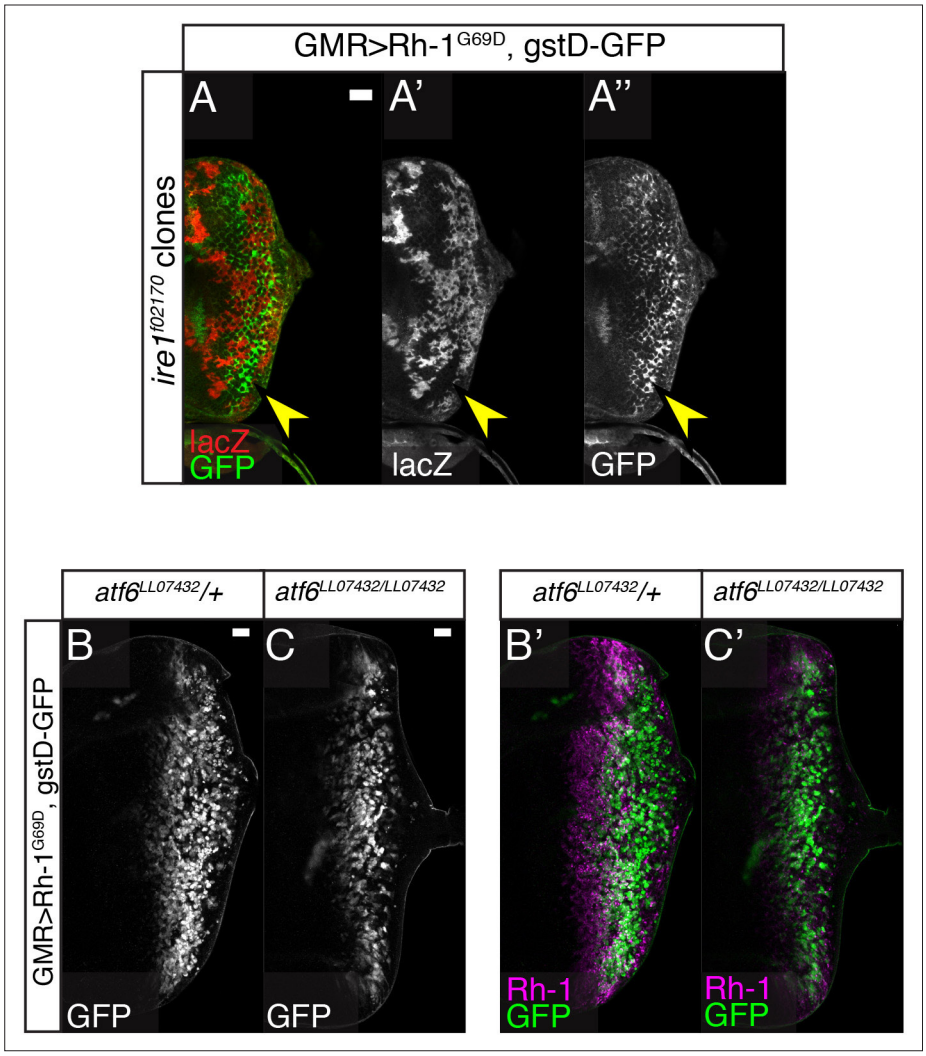

Figure 2—figure supplement 3. *Rh1^{G69D} -induced expression of gstD-GFP neither requires Ire1 nor Atf6.* (**A–C**) *GMR> Rh1^{G69D}* eye discs expressing gstD-GFP (green) in the indicated genetic backgrounds. (**A**) *Ire1^{f02170}* homozygous mutant clones marked by the absence of β Gal expression (red). Note the presence of *gstD-GFP* expression within the mutant clones. Also shown are single channels of β Gal (**A'**) and GFP (**B'**). (**B, C**) *GMR> Rh1^{G69D}* eye discs in *Atf6^{LL07432}* heterozygous (**B**) and homozygous backgrounds (**C**). gstD-GFP single channels (**B, C**) and those merged with anti-Rh1 (magenta) (**B', C'**). Neither *GMR-Gal4> eIF2α^{WT}* (**C**), nor *GMR-Gal4> eIF2α^{51D}* (**D**) activates this reporter.

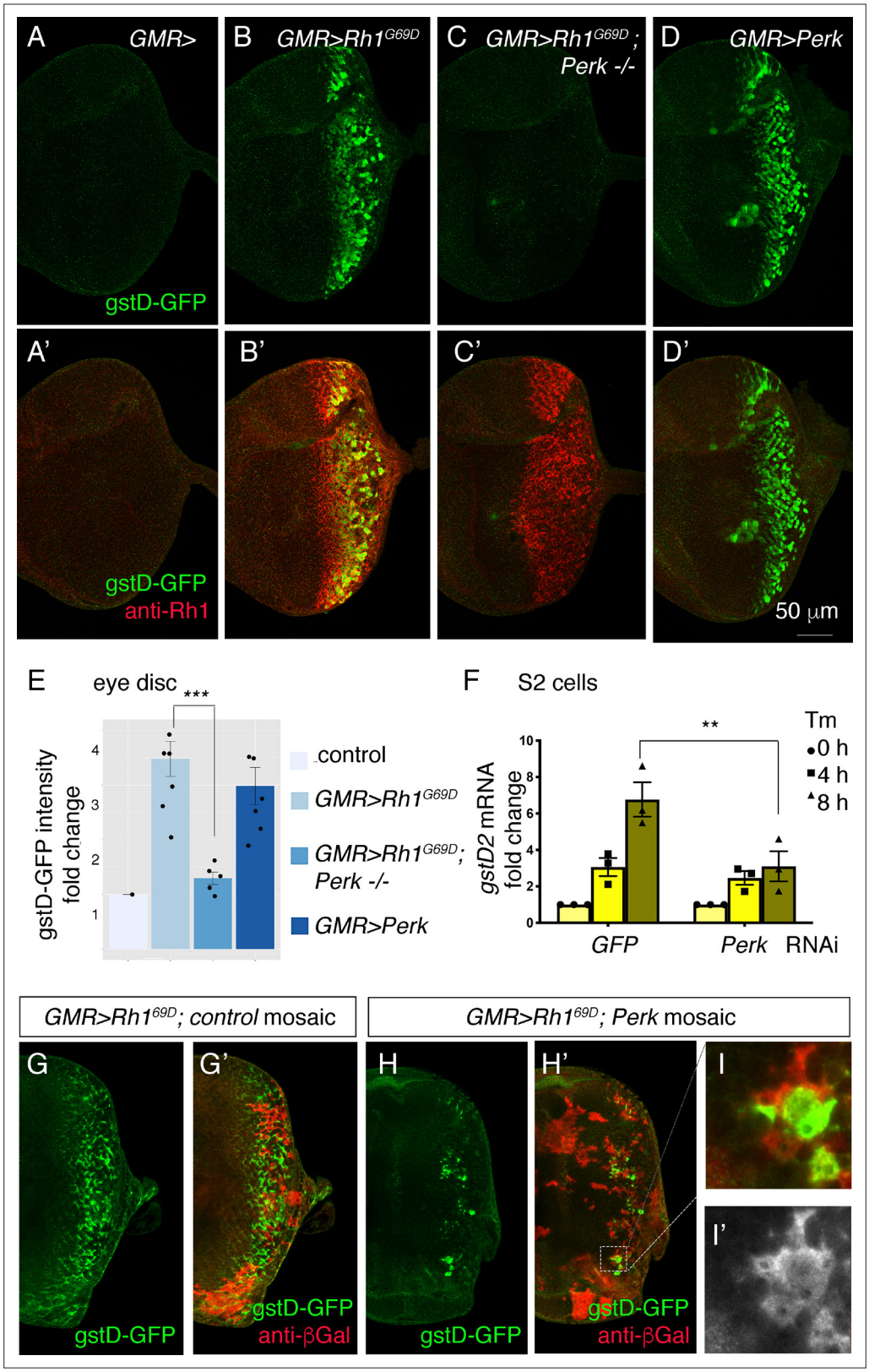

Figure 3. *Perk* is necessary and sufficient to *induce gstD-GFP expression*. (**A–D**) Representative eye imaginal discs with gstD-GFP (green) alone channels (**A–D**), and gstD-GFP (green) channels merged with anti-Rh1 (red) (**A'-D'**). The genotypes of the discs are as follows: (**A**) *GMR-Gal4; gstD-GFP/+*, (**B**) *GMR-Gal4; gstD-GFP/UAS-Rh1^{G69D}*, (**C**) *GMR-Gal4; gstD-GFP/UAS-Rh1^{G69D}; Perk^{e01744}* (**D**) *GMR-Gal4; gstD-GFP/UAS-Perk*. (**E**) Quantification of gstD-GFP

Figure 3 continued on next page

Figure 3 continued

pixel intensity fold change from posterior eye discs of the indicated genotypes from A-D. (**F**) qRT-PCR of *gstD2* normalized to RpL15 in S2 cells treated with 10 ug/mL tunicamycin for 0, 4, or 8 hr. Cells were either pre-treated with control dsRNA (GFP) or those targeting *Perk*. (**G–I**) *gstD-GFP* (green) containing *GMR > Rh1*^{G69D} eye discs with either control mosaic clones (**G**), or those with *Perk* loss-of-function clones (**H, I**). Homozygous *Perk* ^{e01744} clones in H' and I are marked by the absence of β-galactosidase (red) expression. Note that gstD-GFP expression occurs broadly in the background of control mosaic clones, but is largely absent in *Perk* homozygous mutant clones. (**I, I'**) A magnified view of the dotted inset in (**H'**). (**I'**) β-galactosidase only channel (marking *Perk*-positive cells; in white). Scale bar = 50 μm. * = p < 0.05, ** = p < 0.005, *** = p < 0.001.

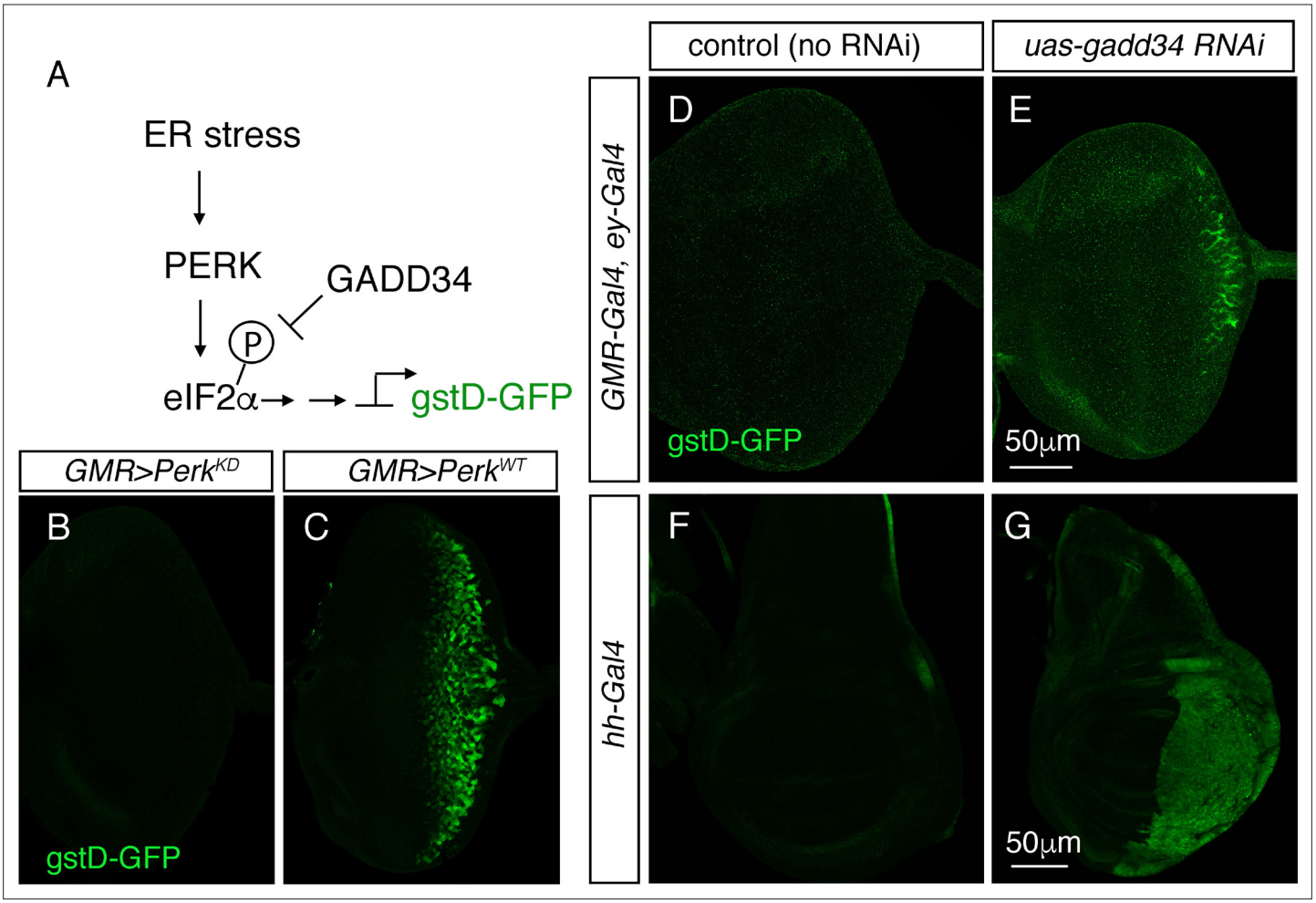

Figure 3—figure supplement 1. PERK's kinase domain and eIF2α phosphorylation mediate *gstD-GFP* induction. (**A**) A schematic diagram of eIF2α phosphorylation regulation. (**B–G**) Late third instar larval imaginal discs expressing *gstD-GFP* (green). Posterior is to the right. (**B–E**) Eye imaginal discs. Expression of a *Perk* transgene with a kinase domain mutation (*Perk*^{KD}) through the *GMR-Gal4* driver does not induce *gstD-GFP* expression (**B**), whereas the *wild type Perk* transgene strongly induces this reporter (**C**). Expression of *gadd34 RNAi* through the *GMR-Gal4, ey-Gal4 drivers* induces *gstD-GFP* at the posterior edge of the eye disc (**E**), whereas gstD-GFP is not detected in the no RNAi control (**D**). (**F, G**) Wing discs. No RNAi control shows low basal levels of *gstD-GFP* expression (**F**), whereas *gadd34 RNAi* expression through the *hh-Gal4* driver induces *gstD-GFP* throughout the domain of Gal4 expression (**G**). Scale bars in E, G = 50 μm.

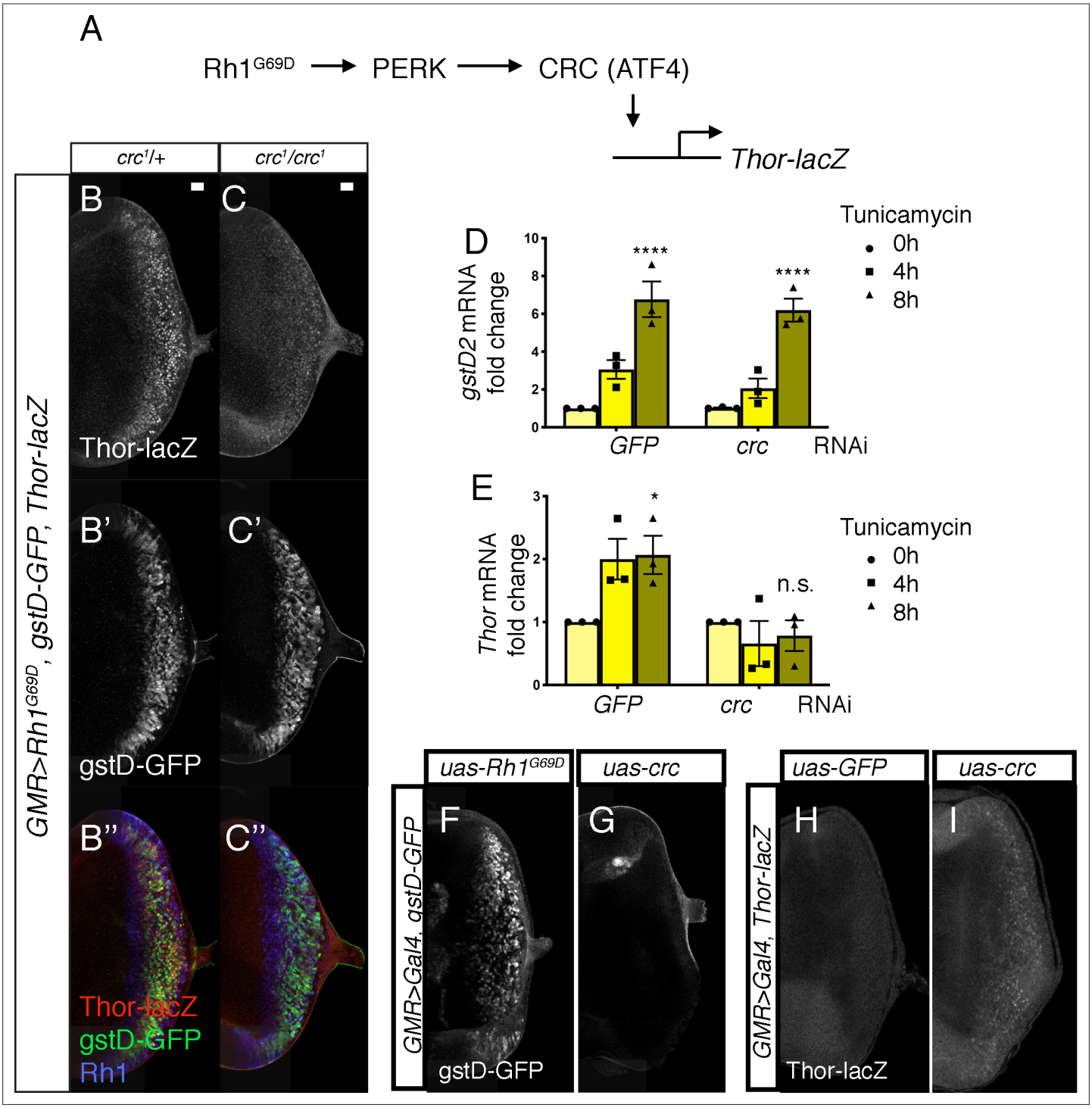

Figure 4. *PERK-mediated gstD expression is ATF4 (crc)-independent.* (**A**) Schematic diagram of the *Drosophila* PERK-ATF4 signaling pathway. CRC is the *Drosophila* ATF4 ortholog, and *Thor-lacZ* is a CRC transcriptional target. (**B, C**) Eye imaginal discs expressing *GMR > Rh1^{G69D}* in either the *crc^{1}/+* control (**B**) or in the *crc^{1}* homozygous backgrounds (**C**). These discs also have *Thor-lacZ* that reports CRC activity (B, C, in white), and *gstD-GFP* (B', C', in white). (**B'', C''**) Images of discs with *Thor-lacZ* (red), *gstD-GFP* (green) and anti-Rh1 (blue) channels merged. Note that *crc^{1}* homozygous mutants block *Thor-lacZ* expression (**C**), but still allows *gstD-GFP* expression in *Rh1^{G69D}* expressing cells (**C', C''**). (**D, E**) qRT-PCR analysis of *gstD2* and *Thor* normalized to *Rpl15* in S2 cells challenged with 10 µg/mL tunicamycin for 0, 4, or 8 hr. Cells were either treated with control dsRNA (GFP) or that target *crc*. (**F, G**) *gstD-GFP* expression (white) in eye discs that are overexpressing either *Rh1^{G69D}* (**F**) or *crc^{leaderless}* (**G**) through the *GMR-Gal4* driver. (**H, I**) *Thor-lacZ* expression (white) in eye discs overexpressing either a control *GFP* transgene (**H**), or *crc^{leaderless}* (**I**) through the *GMR-Gal4* driver. Scale bar = 20 µm. * = $p < 0.05$, **** = $p < 0.0001$. Genotypes: (**B**) *GMR-Gal4; gstD-GFP, crc^{1}/UAS-Rh1^{G69D}, Thor-lacZ.* (**C**) *GMR-Gal4; gstD-GFP, crc^{1}/crc^{1}, UAS-Rh1^{G69D}, Thor-*

Figure 4 continued on next page

Figure 4 continued

lacZ. (**F**) *GMR-Gal4; gstD-GFP/UAS-Rh1^{G69D}*. (**G**) *GMR-Gal4; gstD-GFP/UAS-crc^{leaderless}*. (**H**) *GMR-Gal4; Thor-lacZ/UAS-GFP*. (**I**) *GMR-Gal4; Thor-lacZ/UAS-crc^{leaderless}*.

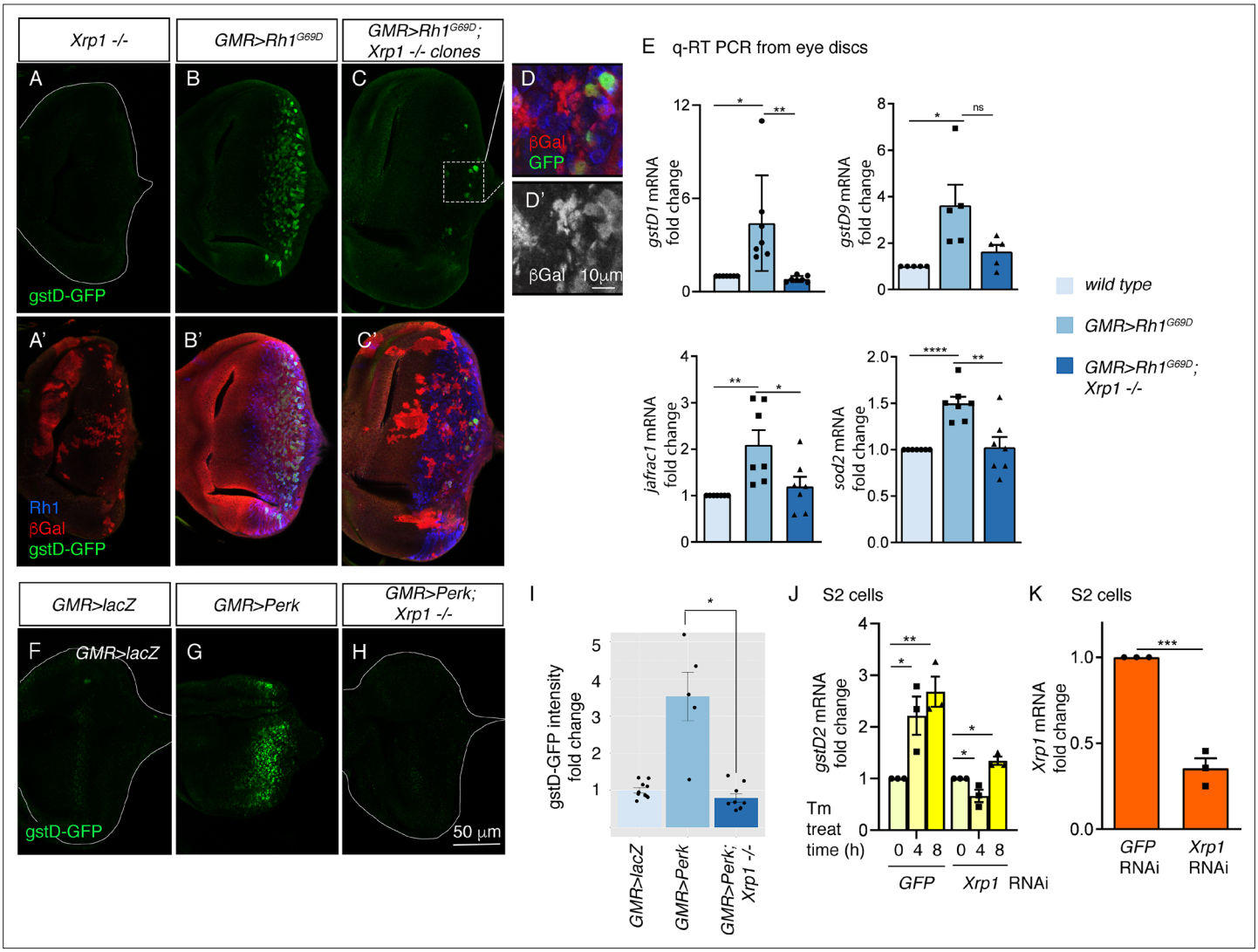

Figure 5. *PERK regulates gstD gene expression through the bZIP transcription factor Xrp1.* (**A–G**) gstD-GFP expression (green) in eye discs. (**A, A'**) An eye disc with homozygous *Xrp1*$^{M2\text{-}73}$ mutant clones that are marked by the absence of β Gal (red). (**B, B'**) A *GMR> Rh1*^{G69D} disc in a control genetic background. (**C, C'**) A *GMR> Rh1*^{G69D} disc with *Xrp1*$^{M2\text{-}73}$ loss-of-function mosaic clones (non-red). (**A–C**) gstD-GFP only channels. (**A'-C'**) Merged images with Rh1 is stained in blue and β gal is in red. Note the absence of *gstD-GFP* in *Xrp1* mutant clones. (**D, D'**) Magnified view of the inset marked in C. The scale bar here represents 10 μm. (**D'**) is the β Gal only channel of the image in (**D**). (**E**) Quantitative(q) RT-PCR results of indicated genes from dissected eye discs. The genotypes are color labeled. (**F–H**) Eye discs expressing control *lacZ* (**E**), *Perk* (**F**), or expressing *Perk* in the background of *Xrp1*$^{M2\text{-}73}$ mosaic clones (**G**). (**I**) Quantification of gstD-GFP intensity fold change in the indicated genotypes. (**J, K**) q RT-PCR results from S2 cells. (**J**) *gstD2* mRNA levels from S2 cells challenged with 10 μg/mL tunicamycin for 0, 4 or 8 hr. The cells were pretreated with dsRNA against either *GFP* (lanes 1–3) or *Xrp1* (lanes 4–6). (**K**) *Xrp1* mRNA levels in cells pretreated with dsRNA against *GFP* or *Xrp1*. All qRT-PCR results were normalized with *Rpl15*. Two tailed t tests were used to assess statistical significance. The scale bar of 50 μm applies to all images except for (**D**). * = p < 0.05, ** = p < 0.005, *** = p < 0.001. Genotypes: (**A**) *GMR-Gal4, ey-FLP; gstD-GFP/+; FRT82, Xrp1*$^{M2\text{-}73}$*/FRT82, arm-lacZ*. (**B**) *GMR-Gal4, ey-FLP; gstD-GFP/UAS-Rh1*^{G69D}. (**C**) *GMR-Gal4, ey-FLP; gstD-GFP/UAS-Rh1*^{G69D}*; FRT82, Xrp1*$^{M2\text{-}73}$*/FRT82, arm-lacZ*. (**E**) *GMR-Gal4, ey-FLP; gstD-GFP/UAS-lacZ*. (**F**) *GMR-Gal4, ey-FLP; gstD-GFP/ UAS-Rh1*^{G69D}. (**G**) *GMR-Gal4, ey-FLP; gstD-GFP/UAS-Rh1*^{G69D}*; FRT82, Xrp1*$^{M2\text{-}73}$*/ FRT82, arm-lacZ*.

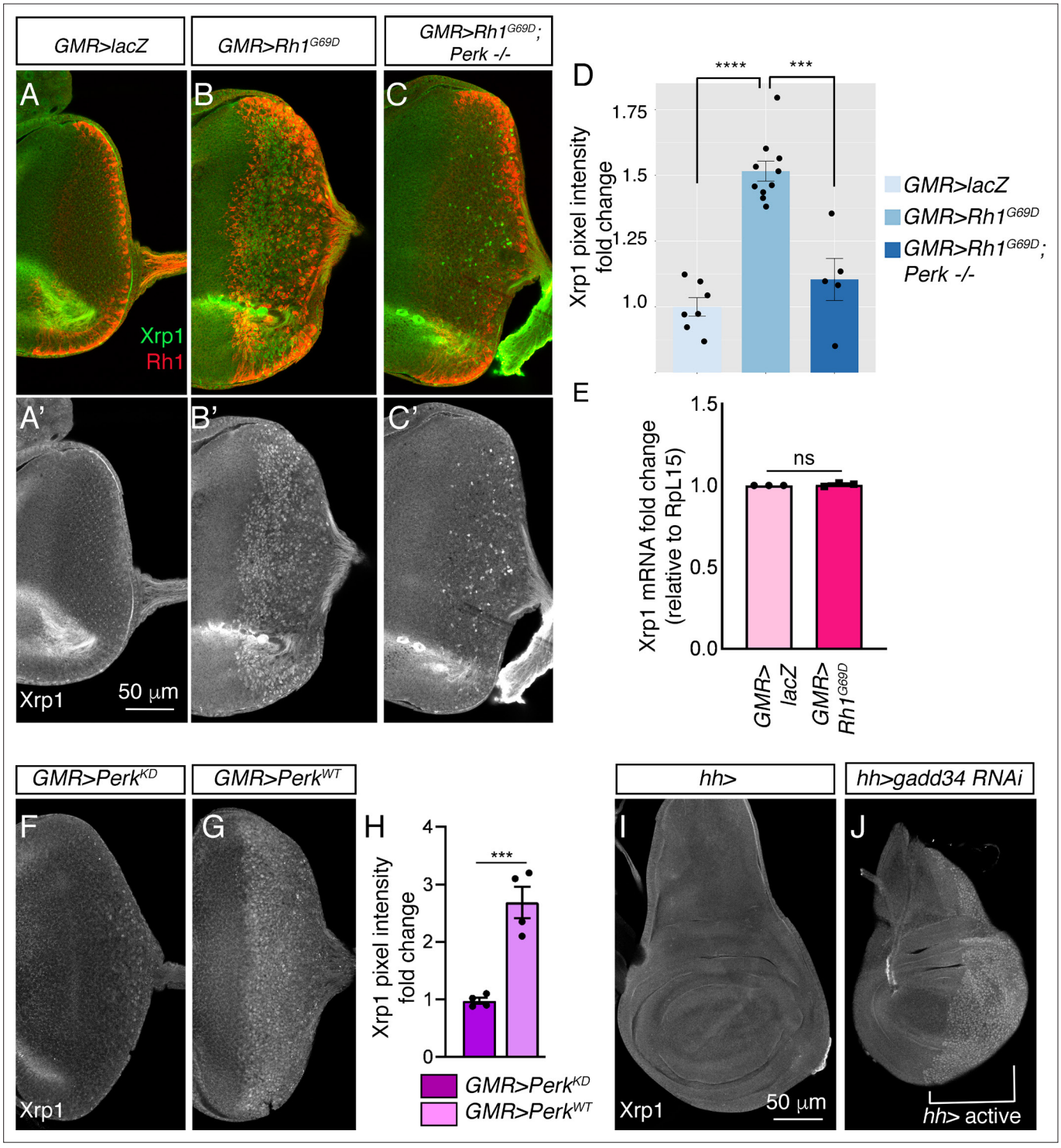

Figure 6. Xrp1 induction is regulated by *Perk* and eIF2α phosphorylation. (**A–C**) Eye discs labeled with anti-Xrp1 (green) and anti-Rh1 (red). (**A'-C'**) Anti-Xrp1 single channels of images in (**A–C**). Genotypes: (**A, A'**) *GMR-Gal4; UAS-lacZ/+*. (**B, B'**) *GMR-Gal4; UAS-Rh1^{G69D}/+*. (**C, C'**) *GMR-Gal4; UAS-Rh1^{G69D}/+; Perk^{e01744}*. The scale bar represents 50 μm. (**D**) Quantification of anti-Xrp1 pixel intensities from eye discs in (**A–D**). (**E**) qRT-PCR analysis of *Xrp1* from *GMR > LacZ* (control) and *GMR > Rh1^{G69D}* eye discs. Xrp1 qRT-PCR results were normalized with that of *Rpl15*. (**F, G**) Anti-Xrp1 immunolabeling (white) in eye imaginal discs. Genotypes: (**F**) *GMR-Gal4; uas-Perk^{KD}*. (**G**) *GMR-Gal4; uas-Perk^{WT}*. (**H**) Quantification of anti-Xrp1 pixel intensities in (**F, G**). (**I, J**) Anti-Xrp1 immunolabeling in wing discs. Genotypes: (**I**) *hh-Gal4/+*. (**J**) *uas-gadd34 RNAi/+; hh-Gal4*. The white bracket indicates the posterior compartment where *hh-Gal4* drives the transgene expression. In all graphs, two tailed t tests were used to assess statistical significance. *** = $p < 0.0005$, **** = $p < 0.00005$ and ns = non-significant, respectively.

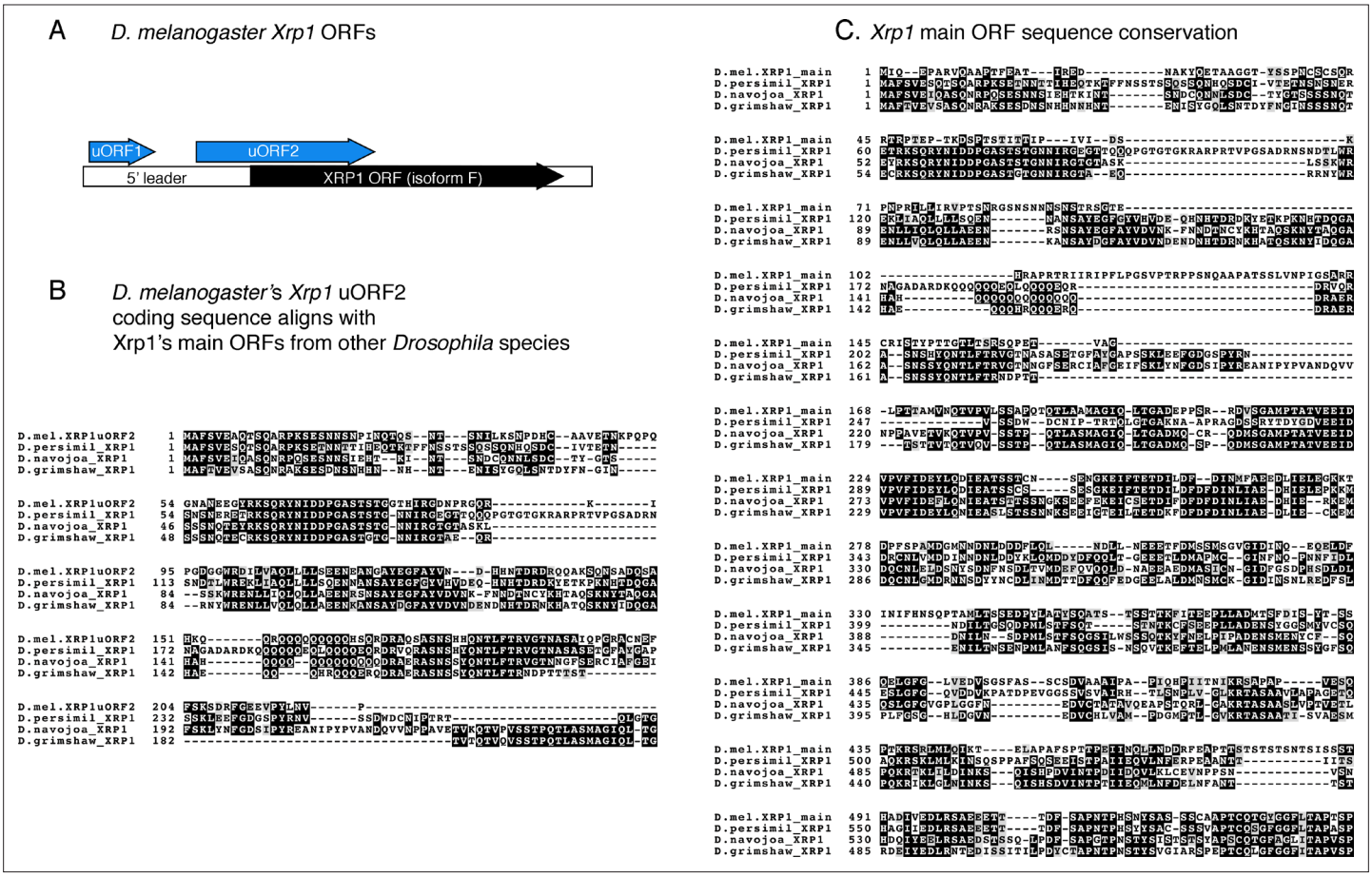

Figure 7. Predicted upstream Open Reading Frames (ORFs) in *Xrp1*. (**A**) A schematic diagram of the predicted ORFs in *D. melanogaster Xrp1*. uORF1 and uORF2 in the 5' leader have initiation start codons with Kozak sequences. uORF1 encodes a peptide of 124 amino acid residues. uORF2 encodes a peptide of 288 amino acid residues. uORF2 overlaps with the main Xrp1 ORF, but is in a different reading frame. (**B**) Amino acid sequence alignment between *D. melanogaster Xrp1* uORF2, and the *Xrp1* main ORFs from the species, *D. persimili, D. navojoa, D. grimshawi*. BoxShade was used for visualizing alignments, with those in black indicating sequence identity. The first 219 residues of the *D. melanogaster Xrp1* uORF2 show high-sequence conservation with the main *Xrp1* ORFs from other species. (**C**) Amino acid sequence alignment between the main ORFs of *D. melanogaster* and other *Drosophila* species. *D. melanogaster*'s *Xrp1* main ORF shows high-sequence conservation with other *Drosophila* species beginning from the 140th amino acid residue.

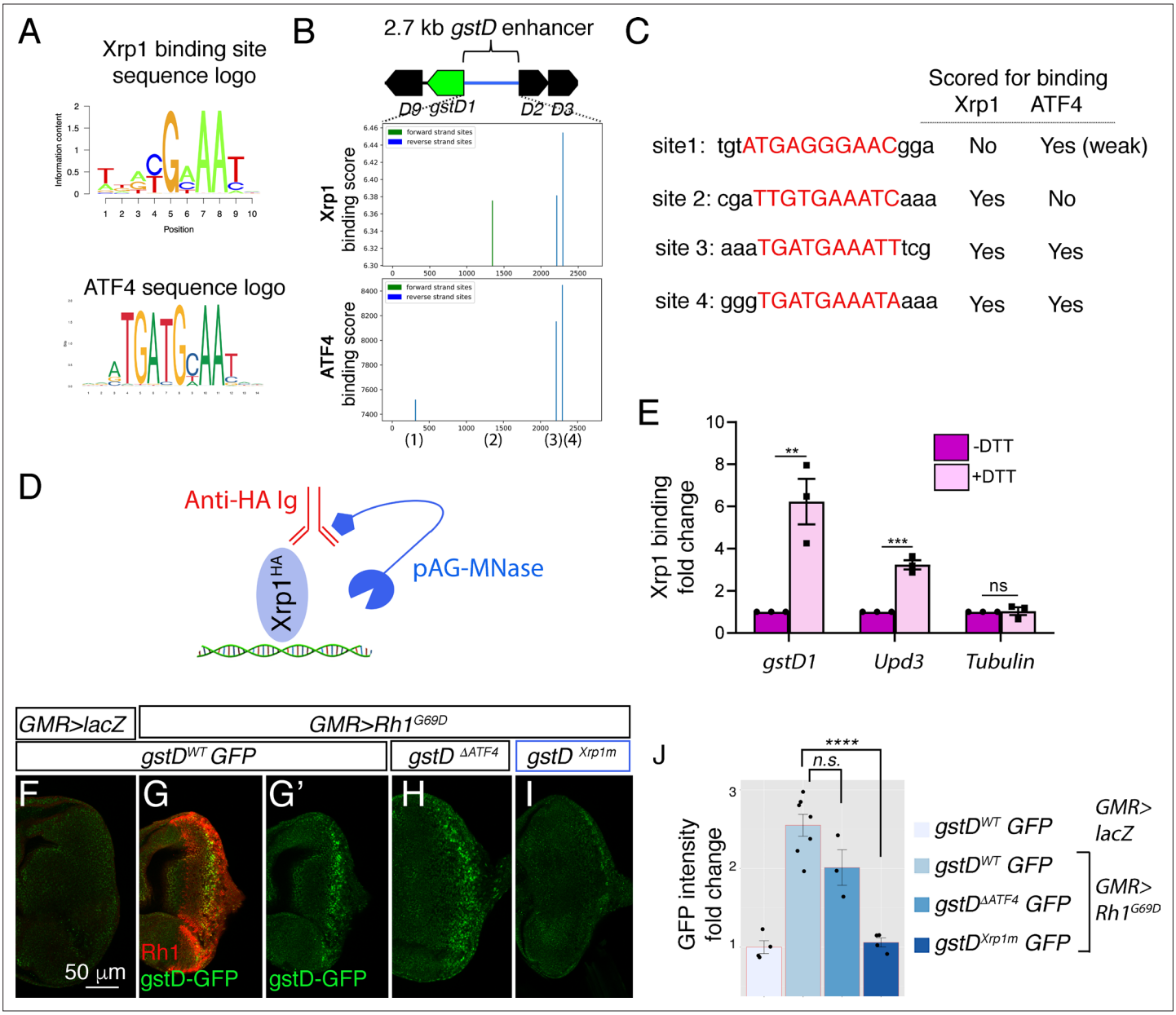

Figure 8. Xrp1 binding sites in the *gstD* enhancer are required for *Rh1*^{G69D} -induced *gstD-GFP* expression. (**A**) Sequence logos representing Xrp1 and ATF4 position frequency matrices. (**B**) Binding score analysis for Xrp1 and ATF4 sites in the *gstD* 2.7 kb enhancer region. Those that score high in the forward strand are depicted in green, whereas those in the reverse strand are shown in blue. The four putative binding sites are numbered below the graphs. (**C**) Putative binding site sequences. The site numbers match those whose positions are indicated in (**B**). (**D**) A schematic diagram of the CUT&RUN approach to assess Xrp1 binding to target DNA. When HA-tagged Xrp1 (light blue) binds to a specific DNA locus, that DNA can be recovered by adding anti-HA antibody (red) and pAG-MNase (dark blue) that cleaves adjacent DNA prior to immunoprecipitation. (**E**) Putative Xrp1 target gene enrichment after Xrp1^{HA} protein pull down as assessed through q-PCR (using CUT&RUN). The y axis shows fold change increases in target gene DNA recovery in response to DTT treatment (normalized to q-PCR values from controls without DTT treatment). (F - J) Representative eye discs either expressing control *lacZ* (**F**) or those expressing *GMR> Rh1*^{G69D} (**G–I**), with variants of the gstD-GFP reporter in green: *gstD WT-GFP* (**F, G**) *gstD* $^{\Delta ATF4}$*-GFP* (**H**) and *gstD* ^{Xrp1m}*-GFP* (**I**). (**G**) shows a merged image with anti-Rh1 (red) and the *gstD-GFP* reporter (green). (**G', H, I**) are gstD-GFP single channel images. (**J**) Quantification of gstD-GFP intensity fold change. Two tailed t tests were used to assess statistical significance. ** = $p < 0.005$, *** = $p < 0.0005$, **** = $p < 0.00001$, n.s. = not significant.